

# Laterobasal Amygdalar Enlargement in 6- to 7-Year-Old Children With Autism Spectrum Disorder

Jieun E. Kim, MD, PhD; In Kyoon Lyoo, MD, PhD, MMS; Annette M. Estes, PhD; Perry F. Renshaw, MD, PhD; Dennis W. Shaw, MD; Seth D. Friedman, PhD; Dajung J. Kim, BA; Sujung J. Yoon, MD, PhD; Jaekuk Hwang, MD, PhD; Stephen R. Dager, MD

**Context:** There is substantial imaging evidence for volumetric abnormalities of the amygdala in younger children with autism spectrum disorder (ASD). The amygdala can be divided into functionally distinct laterobasal, superficial, and centromedial subregions. To date, we are not aware of any *in vivo* reports specifically assessing subregional amygdalar abnormalities in individuals with ASD.

**Objectives:** To evaluate alterations in subregional amygdalar morphology in children with ASD compared with typically developing (TD) children and to examine the relationships with ASD symptom severity.

**Design:** A cross-sectional study encompassing a narrow age range of children with ASD and age-matched TD children that evaluated magnetic resonance imaging–defined subregional morphology of the amygdala using a novel subregional analytic method.

**Setting:** Participants were recruited and clinically evaluated through the University of Washington Autism Center and imaged at the Diagnostic Imaging Sciences Center at the University of Washington. Imaging data were analyzed through the Brain Imaging Laboratory at the Seoul National University.

**Participants:** Fifty-one children 6 to 7 years of age (ASD,  $n=31$  and TD,  $n=20$ ) were assessed using magnetic resonance imaging and behavioral measures.

**Main Outcome Measures:** Volume and subregional measures of the amygdala and measures of social and communication functioning.

**Results:** The ASD group exhibited larger right and left amygdalae, by 12.7% and 11.0%, respectively, relative to the TD group. Subregional analysis revealed that the ASD group had enlarged laterobasal amygdalar subregions, relative to the TD group, after adjusting for age, sex, and hemispheric cerebral volume ( $P < .05$ , false discovery rate corrected and with clustered surface points  $>15$ ). Exploratory analyses revealed that there were linear trends comparing a strictly defined subgroup of children with autistic disorder, who exhibited the greatest extent of laterobasal enlargement, followed by a subgroup of children with pervasive developmental disorder not otherwise specified and then the group of TD children ( $P$  for linear trend  $< .001$ ). There were linear trends between enlargement of laterobasal subregions and lower levels of social and communication functioning ( $P < .001$ ,  $P < .001$ , and  $P = .001$  for 3 areas in the right laterobasal subregion;  $P < .001$  for 1 area in the left laterobasal subregion).

**Conclusion:** The current study demonstrates bilateral enlargement of laterobasal subregions of the amygdala in 6- to 7-year-old children with ASD and that subregional alterations are associated with deficits in social and communicative behavior.

*Arch Gen Psychiatry.* 2010;67(11):1187-1197

**A**UTISM SPECTRUM DISORDER (ASD) is a common neurodevelopmental disorder with a lifetime prevalence of up to 1 in 100 individuals.<sup>1-4</sup> Autism spectrum disorder is typically diagnosed between 2 and 4 years of age based on delayed and atypical language and communication, impaired social interaction, and a restricted range of interests and is associated with functional and financial impacts throughout the individual's life span, as well as substantial distress to families.<sup>5-7</sup> Empirically vali-

dated interventions demonstrate that early intervention can substantially improve the prognosis for many, but not all, children with ASD.<sup>8-10</sup> An enhanced understanding of the neurobiological underpinnings of ASD would promote development of treatments targeting the underlying pathophysiology of this disabling disorder and could extend the benefits of early intervention.<sup>11,12</sup>

Neuroimaging and postmortem studies have reported abnormalities for a number of brain regions in individuals with ASD relative to comparison groups.<sup>13-15</sup>

Author Affiliations are listed at the end of this article.

Among the more consistent findings have been alterations in brain volume,<sup>16-18</sup> frontal lobes,<sup>19,20</sup> cerebellum,<sup>21-23</sup> corpus callosum,<sup>24-26</sup> and amygdala.<sup>17,27-30</sup> Increasingly, there has been an appreciation that brain structural alterations in individuals with ASD may be age related, with the occurrence of volumetric abnormalities, particularly cerebral and amygdalar enlargement, more consistently observed in younger children.<sup>17,30-33</sup> There also have been efforts to characterize subregional anatomical differences in vivo using large-deformation high-dimensional brain mapping methods, which revealed characteristic subregional hippocampal deformations in 3- to 4-year-old children with ASD, predominantly in the vicinity of the subiculum, that are correlated with neuropsychological test results of medial temporal lobe function.<sup>34</sup>

The amygdala may play a pivotal role in the pathophysiology of ASD, since it orchestrates various aspects of social cognition and emotion.<sup>35</sup> Electrophysiological and functional neuroimaging studies in healthy volunteers indicate a crucial role of the amygdala in processing the social signals of body motion, facial expressions, and eye gaze.<sup>36,37</sup> Functional brain imaging studies in individuals with ASD also suggest that core symptoms of ASD are associated with amygdalar dysfunction.<sup>38,39</sup> A study that assessed neuroimaging predictors for the trajectory of social and communicative development in 3- to 4-year-old children with ASD found that amygdalar volume was inversely related to the rate of social and communicative skills development through 6 years of age.<sup>40</sup> Studies of amygdalar anatomy or dysfunction in ASD also more consistently implicate involvement of the right amygdala, although the basis for this observation is not yet established.<sup>17,38,40</sup> Consistent with considerations of age-related anatomical findings in ASD (eTable 1 and eFigure 1, <http://www.archgenpsychiatry.com>), a recent postmortem neuropathological study suggested an early overgrowth of the amygdala in younger children with ASD, followed by a failure to maintain continued growth of the amygdala during later childhood and adolescence.<sup>41</sup>

The amygdala can be divided into laterobasal, superficial, and centromedial subregions having differential arrays of cortical and subcortical connections and thus distinct functional relationships.<sup>42-44</sup> Postmortem studies indicate individuals with ASD have cytoarchitectonic abnormalities in specific amygdalar subregions, mostly involving the lateral nucleus.<sup>41</sup> The laterobasal subregion, which includes the lateral nucleus, has reciprocal projections with widespread brain regions that are associated with reception of sensory information including visual stimuli of facial expression and body posture and auditory stimuli of voices and intonations.<sup>13,45</sup> It also has afferent and efferent connections with various neocortical and striatal brain regions.<sup>13,43,45-53</sup> This wide array of connections is likely to subservise comprehension of social context and help to modulate actions and affective states.<sup>43,54,55</sup> It is, therefore, important to evaluate whether amygdalar volumetric abnormalities in ASD are, to some extent, specific to the laterobasal subregion. To the best of our knowledge, there have not been any prior in vivo studies that examined the subregional specificity of amygdalar volume changes in ASD.

Children with ASD were imaged for the current study at age 6 to 7 years. This group is a subset of children with ASD previously studied at 3 to 4 years of age.<sup>17</sup> Based on our prior findings of amygdalar morphometric differences, and functional relationships to social and communicative development between 3 and 4 and 6 years of age,<sup>17,40</sup> we hypothesized that children with ASD would have enlarged amygdalar volumes and that amygdalar enlargement would be regionally localized to the laterobasal subregion, reflecting its key role in social cognition. High-resolution magnetic resonance images (MRIs) were acquired and analyzed using a novel subregional analytic method using probabilistic subregioning to examine subregional morphometric features of the amygdala. We further examined relationships between the extent of amygdalar subregional enlargement and clinical severity in children with ASD.

## METHODS

### PARTICIPANTS

Thirty-one children with ASD and 20 children with typical development (TD) were evaluated in the current study. The ASD group consisted of 20 children with autistic disorder (AD) (15 boys and 5 girls; mean age, 79.0 months; age range, 73-88 months) and 11 children with pervasive developmental disorder not otherwise specified (PDD-NOS) (9 boys and 2 girls; mean age, 77.5 months; age range, 73-88 months). The TD comparison group consisted of 12 boys and 8 girls (mean age, 78.5 months; age range, 72-94 months). With the exception of 2 subjects new to the study at age 6 years, subjects in the ASD group had entered the study and previously been assessed and scanned at age 3 to 4 years.<sup>17</sup> The ASD and TD groups were matched for chronological age and sex. Children with neurologic disorders, including seizures; physical abnormalities; neurologic impairment in motor or sensory function, including deafness and blindness; or genetically defined disorders (eg, fragile X syndrome), were excluded. Subjects who had any contraindications for MRI, including metal implants or prostheses, were also excluded. Written informed consent, approved by the University of Washington Internal Review Board, was obtained from parents of all participating children.

Diagnosis of ASD was made by experienced clinicians according to criteria in the *DSM-IV*<sup>56</sup> and using the Autism Diagnostic Observation Schedule–Generic<sup>57</sup> and the Autism Diagnostic Interview–Revised.<sup>58</sup> The ASD group was further divided into subgroups of AD and PDD-NOS based on the extent of symptom manifestation, integrating findings from the clinical assessment and the 2 diagnostic instruments, using criteria applied in a consistent manner.<sup>17</sup> Specifically, children in the AD group met criteria for autism on the Autism Diagnostic Observation Schedule–Generic or Autism Diagnostic Interview–Revised (or within 2 points of criteria) and by *DSM-IV*–based clinical assessment. The PDD-NOS diagnosis was made if the child met social criteria for autism on the Autism Diagnostic Interview–Revised but did not meet full criteria in the other symptom domains or was classified as having “ASD” (not AD) on the Autism Diagnostic Observation Schedule–Generic and as having PDD-NOS by *DSM-IV*–based clinical assessment. Adaptive functioning in the domains of communication, socialization, and daily living skills were evaluated in children with ASD using the Vineland Adaptive Behavior Scales (VABS).<sup>59</sup> Intellectual ability was assessed using the Differential Ability Scales–General Conceptual Ability (DAS GCA).<sup>60</sup> The DAS GCA re-

ports scores with a mean (SD) of 100 (15), providing estimates for intelligence level. Among the ASD group, 16 children had scores less than 70 (mean, 52.6; range, 44-68), 14 children had scores more than 70 (mean, 91.8; range, 71-116), and 1 was not assessed with DAS.

A telephone interview with parents was first conducted to screen out a history of learning difficulties, autism spectrum-related difficulties, or the presence of earlier-mentioned exclusionary criteria for those children participating in the TD group. Children who passed this screening were then evaluated directly to further verify TD. The social and communication subscales of the VABS parent interview were assessed for all TD participants. All these scores were in the adequate range or higher (mean [SD] social domain score, 101.1 [11.4]; range, 86-120; mean [SD] communication domain score, 98.5 [9.7]; range, 80-120). A subset of TD children ( $n=13$  with usable MRI data) whose parents agreed to further testing were assessed using the DAS GCA<sup>60</sup> and all were in the average range or higher (mean [SD] score, 116.2 [13.1]; range, 97-137).

## MRI ACQUISITION AND AMYGDALAR TRACING

Detailed procedures for MRI scanning of participants are described in the report of Sparks et al.<sup>17</sup> All participants were studied on the same 1.5-T General Electric Signa scanner (General Electric Medical Systems, Milwaukee, Wisconsin) used at age 3 to 4 years. T1-weighted coronal images with contiguous 1.5-mm slices were obtained using 3-dimensional spoiled gradient echo pulse sequence (repetition time=33 milliseconds, echo time=minimum, 256 × 256 matrix, field of view=22 cm, flip angle=30°). Axial proton density and T2-weighted images were also acquired for inspection of any gross brain abnormalities (repetition time=2000 milliseconds, echo time=13/91 milliseconds, field of view=22 cm, 256 × 160 matrix, slice thickness=2.5 mm, no skip).

Propofol sedation was used for scanning children with ASD whereas TD children were imaged late at night while asleep, which minimized motion artifacts.<sup>61</sup> Most studies had good to excellent image quality with minimal motion artifact according to the Iowa MHCRC image rating scale.<sup>62</sup> After review, data from 2 TD children (2 of 22) were discarded because of inadequate MRI quality.

Manual tracing of the amygdala to produce binary amygdalar images was performed using MEASURE.<sup>40,63</sup> A rater blinded to participants' identity traced the amygdala based on anatomical definition of the amygdala as described by Honeycutt et al.<sup>64</sup> Fifteen cases were traced 3 times by an experienced and trained rater blinded to participants' identity. Intrarater intraclass correlation coefficients were 0.98 and 0.96 for the right and left amygdalae, respectively. Interrater intraclass correlation coefficients with another experienced and trained rater were 0.95 and 0.92 for the right and left amygdalae, respectively.

## SUBREGIONAL ANALYSIS

The 3-dimensional surface of each amygdala was constructed from the 2-dimensional slices of the binary amygdalar images using a marching cube algorithm.<sup>65</sup> Smoothing of the surface was performed with a 3-dimensional Laplacian algorithm.<sup>66</sup>

A 2-step process was used for amygdalar registration. In the first step, the x-, y-, and z-axes of the amygdalae were calculated using principal component analysis. All amygdalae were rotated for these axes to be aligned and translated for the origins of the axes so that the center of inertia was positioned in the same coordinate. In the second step, an iterative closest point algorithm was applied for fine registration. This algorithm registers structures based on local features of the contours. Using the iterative

closest point algorithm, individual amygdalae were registered to an amygdalar template, customized for use in this study by averaging aligned amygdalae from all subjects. This 2-step registration process allowed the matching points of individual amygdalar surfaces to accurately correspond with those of the template amygdala. Because manual correction can be performed in the case of misregistration, during each step the registration process was visually inspected and verified. Among 102 right or left amygdalar image sets, 14 (7 of 62 and 7 of 40 for the ASD and TD groups, respectively;  $\chi^2=0.79$ ;  $P=.37$ ) required manual corrections of principal component analysis alignment.

One thousand surface points were distributed on the surface of the amygdala using spherical mapping methods. Spatial distances from the center of inertia to evenly distributed surface points were measured. Euclidean distances from the center of inertia to surface points of the amygdala, ie, radii of the amygdala, were subjected to statistical modeling. eFigure 2 shows the series of procedures applied for amygdalar shape analysis and methods used to detect subregional differences of the amygdala. This approach provides high sensitivity and specificity for detecting subregional alterations of the amygdala (eAppendix 1, eFigure 3 and eFigure 4, and eTable 2).<sup>67</sup>

The procedure to obtain probabilistic maps for each subregion as a topographical reference was based on stereotaxic probabilistic maps of right and left amygdalar subregions, as described in the Amunts and colleagues report,<sup>68</sup> wherein the amygdalae of 10 postmortem brains were subdivided into laterobasal, superficial, and centromedial subgroups based on microscopic cytoarchitectonic characteristics. The 3-dimensional probabilistic maps for determining each amygdalar subregion are available.<sup>69</sup> These were constructed from digitized histological sections and registered to the standard Montreal Neurological Institute space.<sup>68,70</sup> Using these probabilistic maps, 3-dimensional amygdalar surfaces were reconstructed with an isosurface of 50% probability. This isosurface was affine-transformed to the template amygdala of our sample and then registered to the template amygdala using principal component analysis and iterative closest point. The matrix used in the registration process from the isosurface amygdala to the template amygdala and its reverse matrix were calculated. By overlaying reverse matrix-transformed template amygdalae on the probabilistic maps, the probability that a surface point of the template amygdala belongs to each subregion was calculated. Finally, surface probabilistic maps of our template amygdala were produced as shown in **Figure 1A** and eFigure 5. For the right amygdala, the laterobasal subregion occupied 61% of surface points, 30% superficial and 9% centromedial. For the left amygdala, the laterobasal subregion occupied 53%, 36% superficial and 11% centromedial.

Considering that the normal shape and size of amygdalar subregions in an older population can be different from those of a pediatric subject, we also visualized the boundaries of subregions based on the relative subregional positions and proportions<sup>71</sup> using amygdalar histological sections from the postmortem brain of a 10-year-old who had a sudden cardiac death (Figure 1B). Subregional boundary map findings based on this pediatric brain demonstrate that the relative positions and proportions of the amygdala are similar to those from the adult probabilistic map, except that the relative proportion of the superficial subregion is smaller. Detailed procedures of tissue preparation, staining, and subregion boundary delineation are presented in eAppendix 2 and eFigure 6.

## STATISTICAL ANALYSIS

Independent-sample *t* tests, 2-tailed, were used to compare continuous variables of participants' demographic and clinical char-

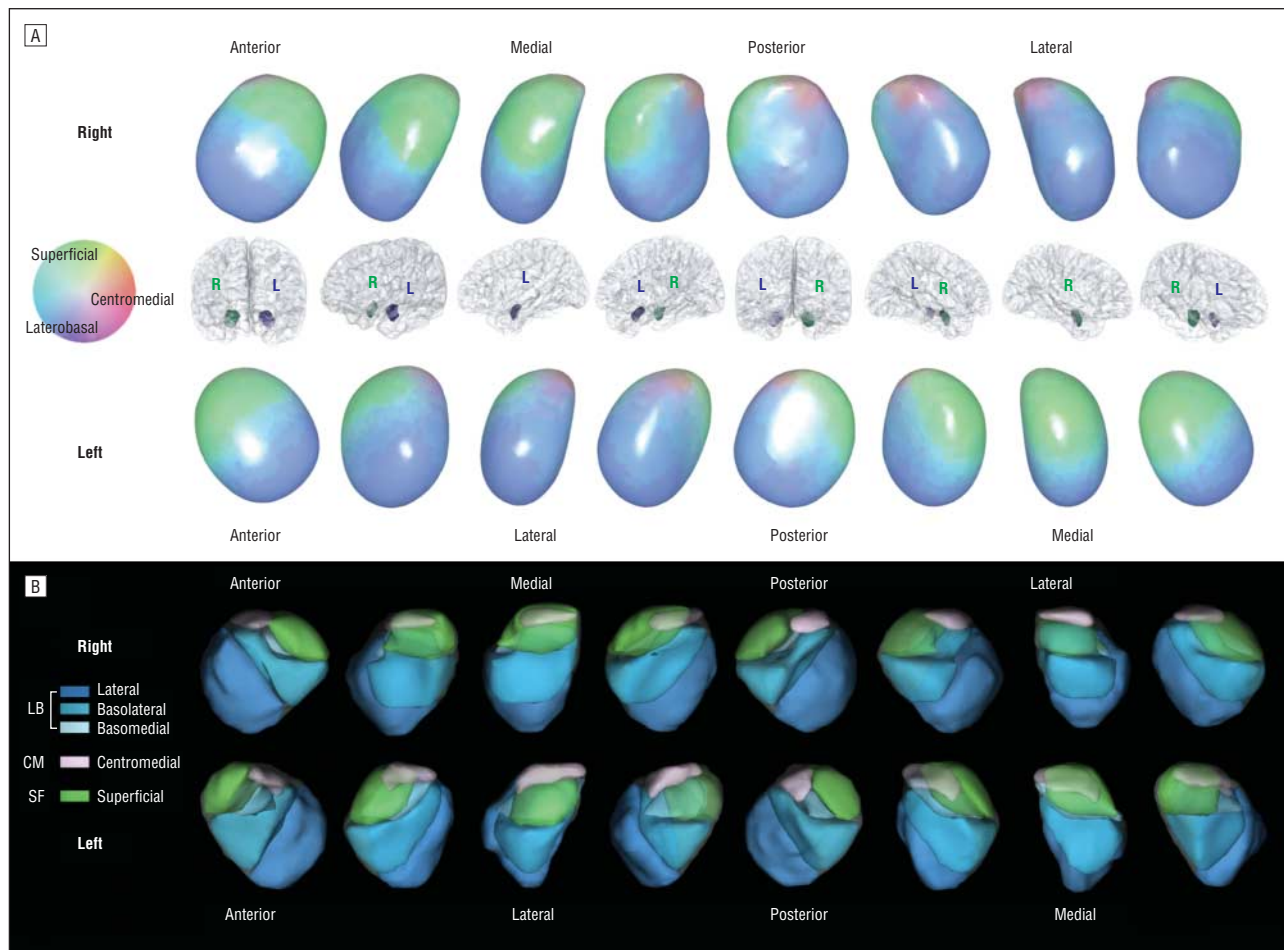


**Figure 1.** Probabilistic maps of laterobasal, superficial, and centromedial amygdalar subregions shown on the template amygdala (A), and 3-dimensional rendering of amygdalar subregions approximated based on subregional divisions of histological amygdalar sections from a pediatric postmortem brain (B). CM indicates centromedial subregion; LB, laterobasal subregion; SF superficial subregion. A, The surface probabilistic maps of 3 amygdalar subregions are shown. Blue represents the laterobasal subregion; green, superficial; and pink, centromedial. Transition areas are expressed as the colors in between blue, green, and pink. The amygdalae are shown being rotated in a 45° clockwise order. For the right amygdala, the laterobasal subregion occupied 61% of surface points, 30% superficial and 9% centromedial. For the left amygdala, the laterobasal subregion occupied 53%, 36% superficial, and 11% centromedial. Probabilistic subregional maps of each subregion are shown in eFigure 2. B, Three-dimensional rendering of amygdalar subregions that were approximated based on subregional divisions at amygdalar histological sections from a postmortem 10-year-old brain. Blue-tone colors represent the laterobasal subregion (within the laterobasal subregion, dark blue indicates the lateral nucleus; blue, basolateral; and light blue, basomedial); green, the superficial subregion; and pink, the centromedial subregion. The amygdalae are shown being rotated in a 45° clockwise order.

acteristics (age and DAS and VABS scores) between ASD and TD groups. A Pearson  $\chi^2$  test was used to assess relationships for sex.

Generalized linear models were used for analyzing between-group differences in amygdalar volume and radii from the center of inertia to surface points. Age, sex, and hemispheric cerebral volume were included as covariates in the model.<sup>72,73</sup> Statistical significance was defined at an  $\alpha$  level less than .05. Multiple comparisons were corrected with false discovery rate.<sup>74</sup> As an additional measure to reduce the chances of false-positive findings, only clusters with more than 15 surface points were retained.<sup>75</sup> The mean radii of the clusters were extracted for further analyses.

Three sets of auxiliary analyses were conducted to assess the potential influence of general cognitive ability. First, DAS GCA levels were covaried to assess between-group subregional morphology differences: subjects were subgrouped as having moderate cognitive impairment (DAS GCA score <50;  $n=7$ ), mild cognitive impairment ( $50 \leq$  DAS GCA score <70;  $n=9$ ), and low/normal cognitive level (DAS GCA score  $\geq$ 70;  $n=34$ ). One child with ASD without assessment with DAS was excluded from this set of analyses. Seven children in the TD group without DAS testing were regarded to belong to the low/

normal cognitive level subgroup based on parent interview and clinician observation. Second, within the ASD and TD groups, areas of significant associations between cognitive ability and radii were analyzed based on the same significance criteria of false discovery rate correction and cluster size thresholding and identified on the template amygdala, after adjusting for age, sex, and hemispheric cerebral volume, to test whether cognitive ability-associated amygdalar areas were distinct from those affected by ASD. To examine whether cognitive ability is differently associated with morphological changes in the TD group as compared with the ASD group, a group  $\times$  DAS GCA score interaction term was tested in the model. Areas with significant interactions were identified on the template amygdala. Third, the extracted mean radii of the clusters with significant group differences were subjected to the model including a group  $\times$  categorized DAS GCA score interaction term as an additional independent variable to test whether there was a significant interaction between diagnostic group and general cognitive ability and whether diagnostic group effects remained significant when accounting for this potential interaction.

Trend analyses<sup>76</sup> were performed to investigate the radii differences of the clusters according to groups of TD children, chil-

**Table. Clinical Characteristics of Participants**

	Mean (SD)		Tests of Significance	
	ASD Group (n = 31)	TD Group (n = 20)	t Test or $\chi^2$ Test	P Value
Male/female, No.	24/7	12/8	$\chi^2 = 1.8$	.18
Age, mo	78.5 (4.5)	78.5 (5.1)	$t_{49} = 0.01$	.99
Differential Ability Scales General Conceptual Ability <sup>a</sup>	70.9 (23.2)	115.6 (13.9)	$t_{41} = 6.4$	<.001
Vineland Adaptive Behavior Scales <sup>a</sup>				
Socialization score	64.2 (10.6)	101.1 (11.4)	$t_{49} = 11.8$	<.001
Communication score	65.2 (20.4)	98.5 (9.7)	$t_{49} = 6.8$	<.001

Abbreviations: ASD, autism spectrum disorder; TD, typically developing.  
<sup>a</sup>Standard scores.

dren with PDD-NOS, and children with AD and to the level of social and communication functioning as measured by VABS. Children with ASD were divided into 2 bitele groups of moderate-level and low-level adaptive functioning groups based on the sum of socialization and communication domain scores of the VABS. Age-, sex-, and hemispheric cerebral volume-corrected residuals for the radii of the clusters were calculated for trend analyses. Statistical significance was defined as an  $\alpha$  level less than .006 to correct for multiple comparisons (8 test sets).

All statistical procedures were performed with Stata version 11 (StataCorp, College Station, Texas). All means are presented with standard deviations.

## RESULTS

Demographic and clinical characteristics of participants are shown in the **Table**. There was no significant age or sex difference between children in the ASD and TD groups.

The ASD group exhibited significantly larger amygdalae bilaterally compared with the TD group, adjusting for age, sex, and hemispheric cerebral volume (right amygdala: 12.7% larger with adjusted values, 15.9% larger unadjusted;  $z = 2.7$ ;  $P = .007$ ; left amygdala: 11.0% larger with adjusted values, 13.8% larger unadjusted;  $z = 3.0$ ;  $P = .003$ ; mean [SD], right amygdala: 1.68 [0.25] cm<sup>3</sup> [ASD] vs 1.45 [0.27] cm<sup>3</sup> [TD]; left amygdala: 1.82 [0.20] cm<sup>3</sup> [ASD] vs 1.60 [0.30] cm<sup>3</sup> [TD]). Hemispheric cerebral volumes were not significantly different between ASD and TD groups (mean [SD], right hemisphere: 614.45 [51.83] cm<sup>3</sup> [ASD] vs 600.95 [45.46] cm<sup>3</sup> [TD]; left hemisphere: 611.57 [51.41] cm<sup>3</sup> [ASD] vs 601.22 [46.65] cm<sup>3</sup> [TD]).

The areas of amygdalar regional enlargement in children with ASD, after adjusting for age, sex, and hemispheric cerebral volume, corresponded primarily to the laterobasal subregions (false discovery rate-corrected  $P < .05$ , cluster surface points  $> 15$ ) (**Figure 2**; 3 clustered areas in the right laterobasal subregion, labeled as area *a*, *b*, and *c*, respectively, and 1 in the left laterobasal subregion, labeled as *d*). Areas of significant enlargement in the right and left amygdalae were 244 and 124 surface points, respectively. To ensure that our findings were robust independent of potential confounders, analyses were repeated with and without covariates of motion artifact rating and sex (eFigure 8).

Results of 3 sets of auxiliary analyses to assess potential confounding effects of general cognitive ability on the

current findings of laterobasal enlargement in ASD are as follows. First, among the 4 areas of *a*, *b*, *c*, and *d* in the laterobasal subregions that were significantly enlarged in the ASD group (Figure 2A), areas *a* and *d*, larger than the other 2 in cluster size, remained significant after accounting for the variance contributed by general cognitive ability. Second, no amygdalar areas were associated with DAS GCA score in the ASD group, using the same significance level of false discovery rate correction and cluster size thresholding as used in comparing ASD and TD groups. In the TD group, some areas in the right amygdala were negatively associated with general cognitive ability levels. However, the areas of significant associations in the TD group (eFigure 9) did not overlap with areas of significant diagnostic group effects of the main analysis shown in Figure 2. The interaction term between DAS GCA score and diagnostic group was also not significant, indicating that no amygdalar areas were differentially affected by general cognitive ability level between groups.

Third, the group  $\times$  DAS GCA score interaction term was not significant in the model. The diagnostic group effect remained significant for 3 areas in the right laterobasal subregion when the group  $\times$  DAS GCA score interaction term was added in the model ( $P = .005$ ,  $P = .02$ , and  $P = .04$ ). For 1 clustered area in the left laterobasal subregion, the diagnostic group effect became nonsignificant when the interaction term was introduced.

The radii from these clustered areas were longest in the AD group and shortest in the TD group; radii in the PDD-NOS group were intermediate in length ( $P$  for linear trend  $< .001$ , adjusting for age, sex, and hemispheric cerebral volume) (**Figure 3**).

There were linear trends suggesting a relationship between greater sizes of these 4 clustered areas in the right and left laterobasal subregions and lower VABS social and communication domain scores, after adjusting for age, sex, and hemispheric cerebral volume ( $P < .001$ ,  $P < .001$ , and  $P = .001$  for 3 sets of areas in the right laterobasal subregion;  $P < .001$  for 1 set of area in the left laterobasal subregion).

## COMMENT

Subregional amygdalar imaging results from this study, analyzed using innovative subregional analytic meth-

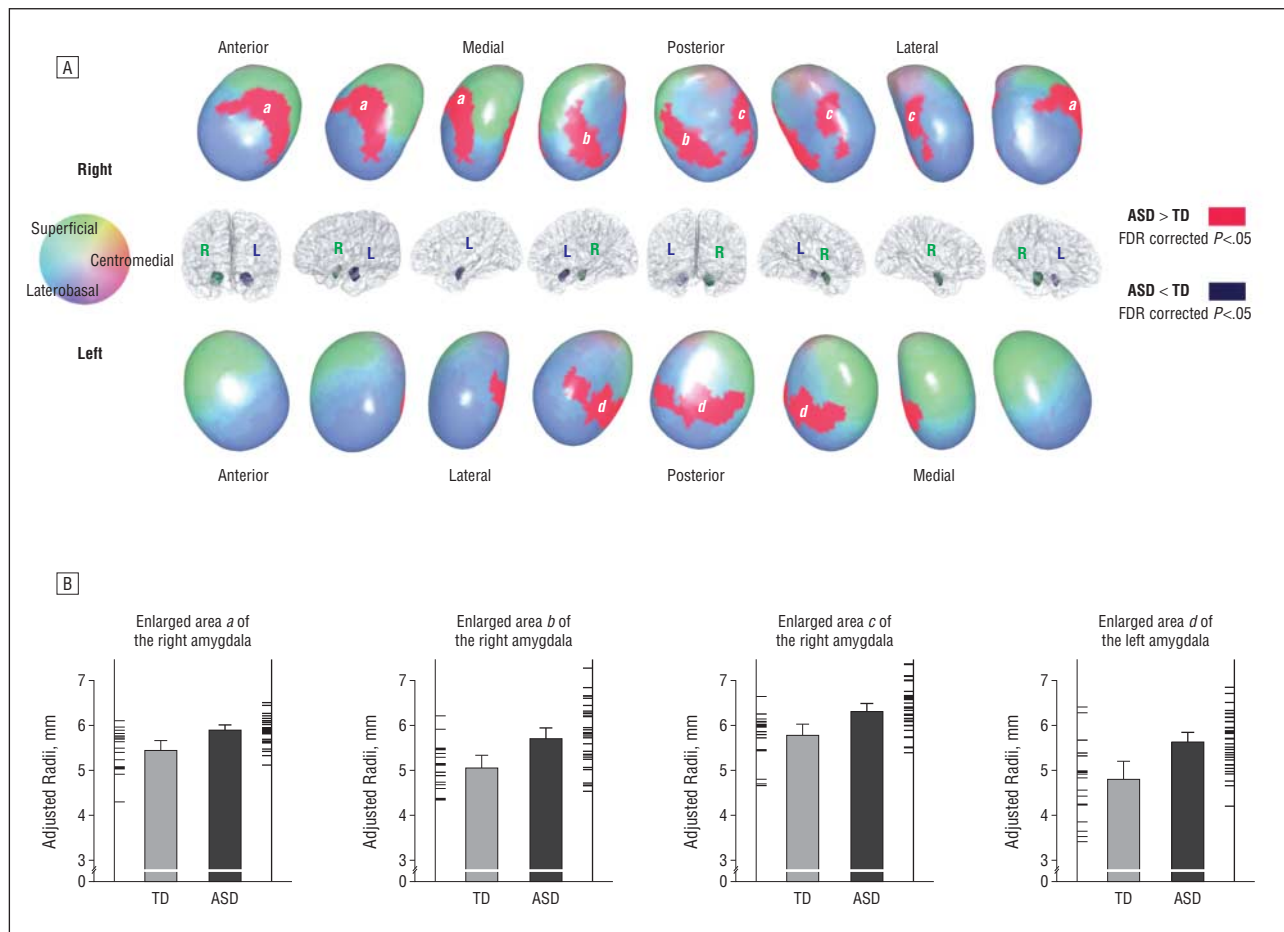


**Figure 2.** Enlarged amygdalar areas in children with autism spectrum disorder (ASD) ( $n=31$ ) compared with typically developing (TD) children ( $n=20$ ) (A) and graphical representations of mean radii for areas of significant group differences (B). A, Areas of greater or smaller amygdalar radii of children with ASD compared with TD children after adjusting for age, sex, and hemispheric cerebral volume (false discovery rate [FDR]-corrected  $P < .05$ , clustered surface points  $> 15$ ) are shown in red and purple, respectively. Enlarged areas were in the laterobasal amygdalar subregions and labeled as *a*, *b*, *c* (right amygdala), and *d* (left amygdala) as shown above. There were no areas of shrinkage in any of 3 amygdalar subregions. The amygdalae are shown being rotated in a 45° clockwise order. B, Mean radii for areas of significant group differences. Radii were adjusted for age, sex, and hemispheric cerebral volume. Gray and black bars denote mean values for TD and ASD groups, respectively. Error bars denote 95% confidence intervals. Gray and black tick marks denote values for each individual in the TD and ASD groups, respectively. Unadjusted mean radii are presented in eFigure 7.

ods, with probabilistic topographical reference for amygdalar subregions, provide the first in vivo evidence, to our knowledge, for specific involvement of the laterobasal subregion underlying amygdalar enlargement in 6- to 7-year-old children with ASD. Comparisons of amygdalar subregional measures demonstrate that areas of enlargement primarily encompass laterobasal subregions of the right and left amygdalae in children with ASD relative to TD children, before and after adjustment for effects of age, sex, and hemispheric cerebral volume (Figure 2). Right laterobasal subregional enlargement was greater in overall size and distribution than in the left amygdala, which is in part in accord with previous reports that suggested more consistent involvement of the right amygdala in individuals with ASD.<sup>17,30-33,40</sup> As was hypothesized based on our prior findings of amygdalar morphometric differences in 3- to 4-year-old children with ASD<sup>17</sup> and functional relationships with the trajectory of social and communicative development through 6 years of age,<sup>40</sup> amygdalar enlargement in the laterobasal subregion was also associated with lower social and communication functional levels.

Extensive analyses to test whether these findings are associated with or driven by general cognitive ability levels indicate that the observed enlargement of the laterobasal amygdalar subregion in the ASD group relative to the TD group is not directly related to this factor and thus is not likely to be associated with cognitive delay. Because our ASD sample is quite different from those reported in many MRI studies<sup>27-29,49,52,77</sup> that generally excluded low-functioning individuals with ASD, our findings may be more generalizable to the ASD population as a whole.

Our most notable finding was that the laterobasal subregion of the right and left amygdalae primarily accounted for overall amygdalar enlargement in 6- to 7-year-old children with ASD relative to TD children. The laterobasal subregion is composed of lateral, basal, and paralaminar nuclei.<sup>46</sup> Assessments of rat and primate amygdalar connections indicate that the lateral nucleus primarily receives major sensory inputs of all modalities from cortical and subcortical regions.<sup>47,78,79</sup> There are substantial intra-amygdaloid connections from the lateral to basal nuclei, through which sensory information

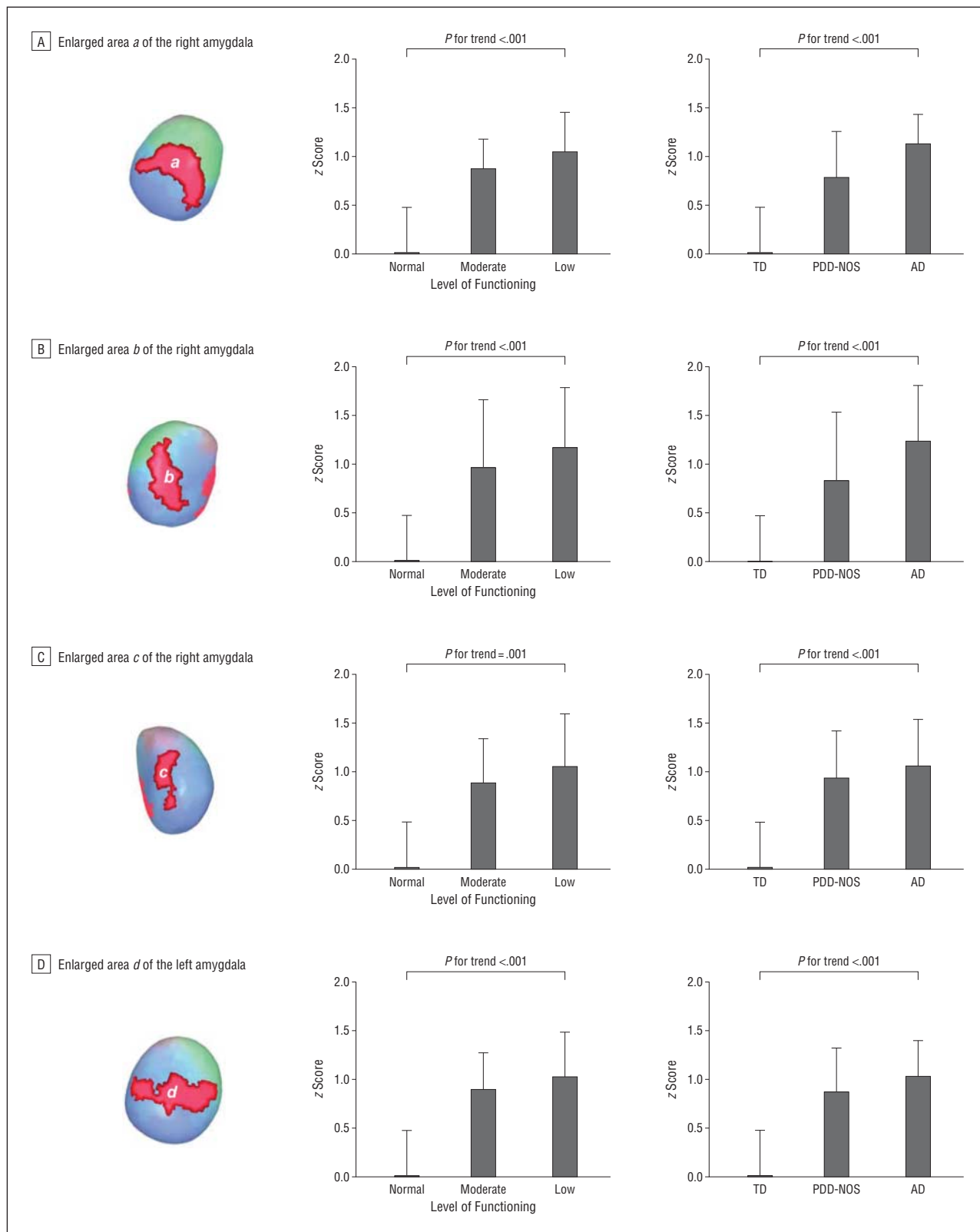


**Figure 3.** Relationships between amygdalar subregional enlargement and autism spectrum disorder clinical severity. AD indicates autistic disorder; PDD-NOS, pervasive developmental disorder not otherwise specified; TD, typically developing. y-Axes denote z scores of residuals (corrected for age, sex, and hemispheric cerebral volume). Solid boxes denote means of z scores while error bars denote 95% confidence intervals. Levels of functioning were determined using the socialization and communication domain scores of the Vineland Adaptive Behavior Scales. Stereotaxic locations of these enlarged areas are shown in Figure 2.

is conveyed.<sup>80</sup> The basal nucleus also receives inputs from the hippocampus and prefrontal cortex and projects to the striatum and cortical areas including the prefrontal

cortex, where social cues are integrated and motor response is executed, to the sensory cortex of temporal and occipital regions and has connections to the central

nucleus.<sup>43,47</sup> The basal nucleus additionally projects to the nucleus accumbens,<sup>51,81</sup> which has an important role in appetitive learning and attachment behavior.<sup>82,83</sup> Although this is a simplified and schematic representation of the complex amygdalar connections with other brain regions, as well as those within the amygdala, it is well in line with our findings that implicate alterations in the laterobasal subregion of the amygdala as a neuroanatomical underpinning for social interaction and communication deficits in ASD.<sup>84</sup> However, to confirm the functional relevance of this amygdalar subregional structural finding in ASD, further studies are needed that combine structural and functional neuroimaging data with amygdalar subregional-level analytic methods.<sup>30,85</sup> The laterobasal subregion of the amygdala has extensive connections with the prefrontal cortex, which modulates the amygdala in a top-down manner. The laterobasal subregion also connects with medial temporal lobe structures, including the hippocampus.<sup>43,46,80</sup> Because an inward deformation of the subiculum in children with ASD compared with TD children was noted when the current cohort was evaluated for hippocampal subregional abnormalities at 3 years of age,<sup>34</sup> it is noteworthy that neurons in the CA1-subiculum border and subiculum have robust connections with the basal nucleus of the amygdala.<sup>53</sup> Speculatively, since neural activity is an important mechanism influencing structural brain development and maturation,<sup>86</sup> altered connectivity between these subregions could influence associated structural development in ASD.

Recent studies have shown that there are genetic risk factors for ASD related to neuronal cell adhesion and synaptic complexity, which is particularly important in the developing brain.<sup>87-89</sup> Cadherin 10 is abundantly expressed in the orbitofrontal and frontal cortex of the human fetal brain, suggesting that these genetic variants might result in dysfunctions in cell adhesion and synapse formations, which are vital for connections with other brain regions.<sup>87</sup> It is intriguing that functional neuroimaging studies in ASD have consistently reported underconnectivity of neural circuits involving the frontal cortex.<sup>90,91</sup> Though very speculative, compromised signals from the frontal cortex in the developing brain may in part be responsible for hyperreactivity of the amygdala, which is also observed in ASD.<sup>38</sup> Amygdalar hyperreactivity at earlier developmental stages may bolster synaptic plasticity<sup>92,93</sup> but subsequently induce overuse atrophy.<sup>41,93</sup> This consideration would be in line with the estimated trajectories of amygdalar volume changes in ASD (eTable 1 and eFigure 1). However, the current study does not provide information that may explain the observed enlargement at a cellular level. There are a number of mechanisms, including proliferation of neurons, glial cells, and astrocytes; impairment of nonfunctioning cell elimination; failed synaptic pruning; or neurofilament increases, that may have resulted in laterobasal subregional enlargement.

Evidence from *ex vivo* human neuropathological studies<sup>41,94</sup> does not provide evidence for a consistent pattern of amygdalar lateral nuclei abnormalities in ASD, but this may in part reflect age effects because brains from older individuals have generally been studied. In post-

mortem studies by Bauman and Kemper,<sup>94</sup> specific pathology of the lateral nucleus was observed only in 2 younger patients with ASD, aged 12 and 21 years, whereas in most cases, other amygdalar nuclei were affected. Although Schumann and Amaral<sup>41</sup> observed a reduced neuron number for the amygdala overall, and the lateral nuclei in particular, for a sample of mostly older adolescents and adults with ASD, neuron numbers in the youngest case study, a 10-year-old with ASD, were reversed, ie, greater numbers, in comparison with the closest age-matched control brain. However, the fact that available postmortem case study subjects are considerably older than children in our study, and the likelihood that in ASD there exists developmental age-specific structural abnormalities of the amygdala (eTable 1 and eFigure 1), precludes further speculation.

There are several limitations of the current study. A modest number of subjects (N=51) raises the possibility of a type II statistical error for specifically implicating alterations of the laterobasal amygdalar subregion in ASD because this is the largest of the 3 amygdalar subregions investigated and our methods might be insensitive to smaller proportional changes of the other subregions. However, results from experiments that modeled comparable phantom amygdalar data with a small mass (24 mm<sup>3</sup>, approximately 1.5% of the TD left amygdalar volume) added to or subtracted from the superficial or centromedial subregions demonstrate high sensitivity for the current subregional analysis method to correctly identify small subregional differences. Detailed procedures of making phantom amygdalar data, testing procedure, and results are presented in eAppendix 1.

Probabilistic maps based on cytoarchitectonic mapping techniques initially developed for more precise anatomical localization of results from functional imaging studies using functional MRI or positron emission tomography<sup>50,68,70,95</sup> are becoming widely applied to structural brain imaging studies for localizing specific brain regions.<sup>96-99</sup> The optimal fit of these maps to study-specific templates is important for accurately localizing the findings.<sup>100,101</sup> In this regard, the 3-dimensional stereotaxic probabilistic maps of right and left amygdalar subregions of Amunts et al<sup>68</sup> that we transformed and used as topographical references are based on the cytoarchitectonic and neuroimaging data of 10 adult postmortem brains. However, the overall shape and the size of amygdalar subregions in an older population can be different from those of a pediatric subject.<sup>102,103</sup> To address this point, a subregional boundary map derived from a 10-year-old postmortem brain and applied as an additional topographic reference showed that using adult subregional maps did not substantively influence interpretation of our findings.

Because the current study is a cross-sectional assessment for a specific and narrow age range, potential influences of age, or an age × diagnosis interaction, on amygdalar morphology could not be examined. At 6 to 7 years of age, amygdalar volumes were larger in the ASD group, even after adjusting for age, sex, and hemispheric cerebral volume. When this ASD cohort was previously evaluated for amygdalar volume differences at 3 to 4 years of age, amygdalar enlargement was proportional to overall



increases in cerebral volume, although disproportionately enlarged for the AD subgroup.<sup>17</sup> Taken together, these observations suggest the possibility that the cerebrum and amygdala may undergo differential developmental trajectories in ASD. Longitudinal studies to compare the growth trajectories between children with ASD and control children for the whole cerebrum, and subcortical regions of interest including the amygdala, are needed to address this complex issue. Future work applying the subregional analysis method to this longitudinal sample may also provide a complimentary approach that could allow us to specifically examine potential age-dependent subregional abnormalities of the amygdala in ASD.

## CONCLUSIONS

We demonstrated amygdalar enlargement in 6- to 7-year-old children with ASD compared with TD children by subregional analyses found to primarily involve enlargement of the laterobasal subregions. This laterobasal subregion of the amygdala is a key structure for sensory information reception, processing, assigning emotional significance, and strategically conveying this information to other effector brain regions, including the prefrontal cortex, hippocampus, and striatum. To further assess the role of amygdalar subregional abnormalities in the pathophysiology of ASD, longitudinal investigation of the dynamic growth trajectory for amygdalar subregions in children with ASD, and in relationship to longitudinal assessment of symptom progression, is warranted.

**Submitted for Publication:** November 22, 2009; final revision received April 16, 2010; accepted May 8, 2010.

**Author Affiliations:** Department of Psychiatry and Interdisciplinary Program in Neuroscience, Seoul National University (Drs J. E. Kim and Lyoo and Ms D. J. Kim), Department of Psychiatry, Catholic University of Korea (Dr Yoon), and Department of Psychiatry, Soonchunhyang University College of Medicine (Dr Hwang), Seoul, South Korea; The Brain Institute, University of Utah, Salt Lake City (Drs Lyoo and Renshaw); and Departments of Speech and Hearing Sciences (Dr Estes) and Radiology (Drs Shaw, Friedman, and Dager), University of Washington, and University of Washington Autism Center (Drs Estes and Dager), Seattle.

**Correspondence:** In Kyoonyoung Lyoo, MD, PhD, MMS, Department of Psychiatry and Interdisciplinary Program in Neuroscience, Seoul National University, 28 Yongong-dong, Jongno-gu, Seoul 110-744, South Korea (inkylyoo@gmail.com) and Stephen R. Dager, MD, Department of Radiology, University of Washington School of Medicine, 1100 NE 45th St, Ste 555, Seattle, WA 98105 (srd@u.washington.edu).

**Author Contributions:** Drs Lyoo and Dager had full access to all of the data in the study and take responsibility for the integrity of the data and the accuracy of the data analysis.

**Financial Disclosure:** Dr Lyoo has received research support from Eli Lilly, GlaxoSmithKline, Lundbeck, and AstraZeneca. Dr Renshaw has been a consultant to Novar-

tis, Roche, and Kyowa Hakko and has received research support from Roche, GlaxoSmithKline, and Eli Lilly.

**Funding/Support:** This research was supported by grants U19HD34565, P50HD066782, P50HD055782, and R01HD-55741 from the National Institute of Child Health and Human Development to the University of Washington (Dr Dager), grant U54MH066399 from the National Institute of Mental Health (Dr Dager), Independent Investigator Awards from the National Alliance for Research on Schizophrenia and Depression (Drs Lyoo and Renshaw), Young Investigator Award from the National Alliance for Research on Schizophrenia and Depression (Dr Hwang), grant 2009-0074584 from the Basic Science Research Program through the National Research Foundation of Korea (Dr J. E. Kim) funded by the Ministry of Education, Science, and Technology, grant 03-2007-018-0 from the Seoul National University Hospital Research Fund (Dr Lyoo), grant KRF-2008-220-E00021 from the Korea Research Foundation funded by the Korean Government (Dr Lyoo), and grant 2009K001272 from the Brain Research Center of the 21st Century Frontier Research Program funded by the Korean Ministry of Education, Science, and Technology (Dr Lyoo).

**Role of the Sponsors:** The sponsors had no role in the collection, management, analysis, or interpretation of the data and had no role in the preparation, review, or approval of the manuscript.

**Online-Only Material:** The eAppendixes, eTables, and eFigures are available at <http://www.archgenpsychiatry.com>.

**Additional Contributions:** Sujin Bae, MS, assisted in preprocessing amygdalar data; Han Byul Cho, BS, assisted in preprocessing phantom data sets; Jaeyoun Pyun, BA, Hyeonseok S. Jeong, BS, and Bobbi F. Sparks, BA, provided technical support; and Hengjun Kim, PhD, and Namkug Kim, PhD, performed earlier code writing for part of the software used. We thank Suk-Woo Choi, PhD, for valuable discussions.

## REFERENCES

- Centers for Disease Control and Prevention. Prevalence of autism spectrum disorders: Autism and Developmental Disabilities Monitoring Network, 14 sites, United States, 2002. *MMWR Morb Mortal Wkly Rep*. 2007;56(suppl 01):12-28. <http://www.cdc.gov/mmwr/preview/mmwrhtml/ss5601a2.htm>. Accessed October 29, 2009.
- Yeargin-Allsopp M, Rice C, Karapurkar T, Doernberg N, Boyle C, Murphy C. Prevalence of autism in a US metropolitan area. *JAMA*. 2003;289(1):49-55.
- Kogan MD, Blumberg SJ, Schieve LA, Boyle CA, Perrin JM, Ghandour RM, Singh GK, Strickland BB, Trevathan E, van Dyck PC. Prevalence of parent-reported diagnosis of autism spectrum disorder among children in the US, 2007. *Pediatrics*. 2009;124(5):1395-1403.
- Baird G, Simonoff E, Pickles A, Chandler S, Loucas T, Meldrum D, Charman T. Prevalence of disorders of the autism spectrum in a population cohort of children in South Thames: the Special Needs and Autism Project (SNAP). *Lancet*. 2006;368(9531):210-215.
- Howlin P, Goode S, Hutton J, Rutter M. Adult outcome for children with autism. *J Child Psychol Psychiatry*. 2004;45(2):212-229.
- Ganz ML. The lifetime distribution of the incremental societal costs of autism. *Arch Pediatr Adolesc Med*. 2007;161(4):343-349.
- Estes AM, Munson J, Dawson G, Koehler E, Zhou XH, Abbott R. Parenting stress and psychological functioning among mothers of preschool children with autism and developmental delay. *Autism*. 2009;13(4):375-387.
- Rogers SJ, Vismara LA. Evidence-based comprehensive treatments for early autism. *J Clin Child Adolesc Psychol*. 2008;37(1):8-38.

9. Lovaas OI. Behavioral treatment and normal educational and intellectual functioning in young autistic children. *J Consult Clin Psychol.* 1987;55(1):3-9.
10. Smith T, Groen AD, Wynn JW. Randomized trial of intensive early intervention for children with pervasive developmental disorder. *Am J Ment Retard.* 2000;105(4):269-285.
11. Petrovic P, Kalisch R, Singer T, Dolan RJ. Oxytocin attenuates affective evaluations of conditioned faces and amygdala activity. *J Neurosci.* 2008;28(26):6607-6615.
12. Dawson G. Early behavioral intervention, brain plasticity, and the prevention of autism spectrum disorder. *Dev Psychopathol.* 2008;20(3):775-803.
13. Amaral DG, Schumann CM, Nordahl CW. Neuroanatomy of autism. *Trends Neurosci.* 2008;31(3):137-145.
14. DiCicco-Bloom E, Lord C, Zwaigenbaum L, Courchesne E, Dager SR, Schmitz C, Schultz RT, Crawley J, Young LJ. The developmental neurobiology of autism spectrum disorder. *J Neurosci.* 2006;26(26):6897-6906.
15. Brambilla P, Hardan A, di Nemi SU, Perez J, Soares JC, Barale F. Brain anatomy and development in autism: review of structural MRI studies. *Brain Res Bull.* 2003;61(6):557-569.
16. Courchesne E, Carper R, Akshoomoff N. Evidence of brain overgrowth in the first year of life in autism. *JAMA.* 2003;290(3):337-344.
17. Sparks BF, Friedman SD, Shaw DW, Aylward EH, Echelard D, Artru AA, Maravilla KR, Giedd JN, Munson J, Dawson G, Dager SR. Brain structural abnormalities in young children with autism spectrum disorder. *Neurology.* 2002;59(2):184-192.
18. Hazlett HC, Poe M, Gerig G, Smith RG, Provenzale J, Ross A, Gilmore J, Piven J. Magnetic resonance imaging and head circumference study of brain size in autism: birth through age 2 years. *Arch Gen Psychiatry.* 2005;62(12):1366-1376.
19. Carper RA, Courchesne E. Localized enlargement of the frontal cortex in early autism. *Biol Psychiatry.* 2005;57(2):126-133.
20. Hazlett HC, Poe MD, Gerig G, Smith RG, Piven J. Cortical gray and white brain tissue volume in adolescents and adults with autism. *Biol Psychiatry.* 2006;59(1):1-6.
21. Courchesne E, Yeung-Courchesne R, Press GA, Hesselink JR, Jernigan TL. Hypoplasia of cerebellar vermal lobules VI and VII in autism. *N Engl J Med.* 1988;318(21):1349-1354.
22. Hardan AY, Minshew NJ, Harenski K, Keshavan MS. Posterior fossa magnetic resonance imaging in autism. *J Am Acad Child Adolesc Psychiatry.* 2001;40(6):666-672.
23. Webb SJ, Sparks BF, Friedman SD, Shaw DW, Giedd J, Dawson G, Dager SR. Cerebellar vermal volumes and behavioral correlates in children with autism spectrum disorder. *Psychiatry Res.* 2009;172(1):61-67.
24. Piven J, Bailey J, Ranson BJ, Arndt S. An MRI study of the corpus callosum in autism. *Am J Psychiatry.* 1997;154(8):1051-1056.
25. Hardan AY, Minshew NJ, Keshavan MS. Corpus callosum size in autism. *Neurology.* 2000;55(7):1033-1036.
26. Boger-Megiddo I, Shaw DW, Friedman SD, Sparks BF, Artru AA, Giedd JN, Dawson G, Dager SR. Corpus callosum morphometrics in young children with autism spectrum disorder. *J Autism Dev Disord.* 2006;36(6):733-739.
27. Aylward EH, Minshew NJ, Goldstein G, Honeycutt NA, Augustine AM, Yates KO, Barta PE, Pearson GD. MRI volumes of amygdala and hippocampus in nonmentally retarded autistic adolescents and adults. *Neurology.* 1999;53(9):2145-2150.
28. Abell F, Krams M, Ashburner J, Passingham R, Friston K, Frackowiak R, Happé F, Frith C, Frith U. The neuroanatomy of autism: a voxel-based whole brain analysis of structural scans. *Neuroreport.* 1999;10(8):1647-1651.
29. Howard MA, Cowell PE, Boucher J, Brooks P, Mayes A, Farrant A, Roberts N. Convergent neuroanatomical and behavioural evidence of an amygdala hypothesis of autism. *Neuroreport.* 2000;11(13):2931-2935.
30. Mosconi MW, Cody-Hazlett H, Poe MD, Gerig G, Gimpel-Smith R, Piven J. Longitudinal study of amygdala volume and joint attention in 2- to 4-year-old children with autism. *Arch Gen Psychiatry.* 2009;66(5):509-516.
31. Aylward EH, Minshew NJ, Field K, Sparks BF, Singh N. Effects of age on brain volume and head circumference in autism. *Neurology.* 2002;59(2):175-183.
32. Courchesne E, Karns CM, Davis HR, Ziccardi R, Carper RA, Tigue ZD, Chisum HJ, Moses P, Pierce K, Lord C, Lincoln AJ, Pizzo S, Schreibman L, Haas RH, Akshoomoff NA, Courchesne RY. Unusual brain growth patterns in early life in patients with autistic disorder: an MRI study. *Neurology.* 2001;57(2):245-254.
33. Schumann CM, Hamstra J, Goodlin-Jones BL, Lotspeich LJ, Kwon H, Buonocore MH, Lammers CR, Reiss AL, Amaral DG. The amygdala is enlarged in children but not adolescents with autism; the hippocampus is enlarged at all ages. *J Neurosci.* 2004;24(28):6392-6401.
34. Dager SR, Wang L, Friedman SD, Shaw DW, Constantino JN, Artru AA, Dawson G, Csernansky JG. Shape mapping of the hippocampus in young children with autism spectrum disorder. *AJNR Am J Neuroradiol.* 2007;28(4):672-677.
35. Baron-Cohen S, Ring HA, Bullmore ET, Wheelwright S, Ashwin C, Williams SC. The amygdala theory of autism. *Neurosci Biobehav Rev.* 2000;24(3):355-364.
36. Morris JS, Ohman A, Dolan RJ. Conscious and unconscious emotional learning in the human amygdala. *Nature.* 1998;393(6684):467-470.
37. Oya H, Kawasaki H, Howard MA III, Adolphs R. Electrophysiological responses in the human amygdala discriminate emotion categories of complex visual stimuli. *J Neurosci.* 2002;22(21):9502-9512.
38. Dalton KM, Nacewicz BM, Johnstone T, Schaefer HS, Gernsbacher MA, Goldsmith HH, Alexander AL, Davidson RJ. Gaze fixation and the neural circuitry of face processing in autism. *Nat Neurosci.* 2005;8(4):519-526.
39. Kleinhans NM, Richards T, Sterling L, Stegbauer KC, Mahurin R, Johnson LC, Greenon J, Dawson G, Aylward E. Abnormal functional connectivity in autism spectrum disorders during face processing. *Brain.* 2008;131(pt 4):1000-1012.
40. Munson J, Dawson G, Abbott R, Faja S, Webb SJ, Friedman SD, Shaw DW, Artru A, Dager SR. Amygdalar volume and behavioral development in autism. *Arch Gen Psychiatry.* 2006;63(6):686-693.
41. Schumann CM, Amaral DG. Stereological analysis of amygdala neuron number in autism. *J Neurosci.* 2006;26(29):7674-7679.
42. Sakamoto N, Pearson J, Shinoda GF, Alheid GF, de Olmos JS, Heimer L. The human basal forebrain. In: Bloom FE, Bjorklund A, Hokfelt T, eds. *The Primate Nervous System. Part III.* Amsterdam, the Netherlands: Elsevier; 1999:57-226.
43. Aggleton JP. *The Amygdala: A Functional Analysis.* 2nd ed. New York, NY: Oxford University Press; 2000.
44. Passingham RE, Stephan KE, Kötter R. The anatomical basis of functional localization in the cortex. *Nat Rev Neurosci.* 2002;3(8):606-616.
45. Swanson LW, Petrovich GD. What is the amygdala? *Trends Neurosci.* 1998;21(8):323-331.
46. Whalen PJ, Phelps EA. *The Human Amygdala.* New York, NY: The Guilford Press; 2009.
47. LeDoux J. The amygdala. *Curr Biol.* 2007;17(20):R868-R874.
48. Baillone BW, Killcross S. Parallel incentive processing: an integrated view of amygdala function. *Trends Neurosci.* 2006;29(5):272-279.
49. Dziobek I, Bahnemann M, Convit A, Heekeren HR. The role of the fusiform-amygdala system in the pathophysiology of autism. *Arch Gen Psychiatry.* 2010;67(4):397-405.
50. Roy AK, Shehzad Z, Margulies DS, Kelly AM, Uddin LQ, Gotimer K, Biswal BB, Castellanos FX, Milham MP. Functional connectivity of the human amygdala using resting state fMRI. *Neuroimage.* 2009;45(2):614-626.
51. Russchen FT, Bakst I, Amaral DG, Price JL. The amygdalostriatal projections in the monkey: an anterograde tracing study. *Brain Res.* 1985;329(1-2):241-257.
52. Corbett BA, Carmean V, Ravizza S, Wendelken C, Henry ML, Carter C, Rivera SM. A functional and structural study of emotion and face processing in children with autism. *Psychiatry Res.* 2009;173(3):196-205.
53. Rosene DL, Van Hoesen GW. Hippocampal efferents reach widespread areas of cerebral cortex and amygdala in the rhesus monkey. *Science.* 1977;198(4314):315-317.
54. Hoffman KL, Gothard KM, Schmid MC, Logothetis NK. Facial-expression and gaze-selective responses in the monkey amygdala. *Curr Biol.* 2007;17(9):766-772.
55. Hurlmann R, Rehme AK, Diesse M, Kukolja J, Maier W, Walter H, Cohen MX. Segregating intra-amygdalar responses to dynamic facial emotion with cytoarchitectonic maximum probability maps. *J Neurosci Methods.* 2008;172(1):13-20.
56. American Psychiatric Association. *Diagnostic and Statistical Manual of Mental Disorders.* 4th ed. Washington, DC: American Psychiatric Press; 1994.
57. Lord C, Risi S, Lambrecht L, Cook EH Jr, Leventhal BL, DiLavore PC, Pickles A, Rutter M. The Autism Diagnostic Observation Schedule-Generic: a standard measure of social and communication deficits associated with the spectrum of autism. *J Autism Dev Disord.* 2000;30(3):205-223.
58. Lord C, Rutter M, Le Couteur A. Autism Diagnostic Interview-Revised: a revised version of a diagnostic interview for caregivers of individuals with possible pervasive developmental disorders. *J Autism Dev Disord.* 1994;24(5):659-685.
59. Sparrow SS, Balla DA, Cicchetti D. *Vineland Adaptive Behavior Scales.* Circle Pines, MN: American Guidance Service Inc; 1984.
60. Elliott CD. *Differential Ability Scales (DAS).* San Antonio, TX: Psychological Corp; 1990.
61. Amundsen LB, Artru AA, Dager SR, Shaw DW, Friedman S, Sparks B, Dawson G. Propofol sedation for longitudinal pediatric neuroimaging research. *J Neurosurg Anesthesiol.* 2005;17(4):180-192.

62. Iowa Mental Health Clinical Research Center. MHCRC web rater. [http://www.psychiatry.uiowa.edu/mhcr/IPLpages/qa\\_main.htm](http://www.psychiatry.uiowa.edu/mhcr/IPLpages/qa_main.htm). Accessed April 13, 2009.
63. Barta PE, Dhingra L, Royall R, Schwartz E. Improving stereological estimates for the volume of structures identified in three-dimensional arrays of spatial data. *J Neurosci Methods*. 1997;75(2):111-118.
64. Honeycutt NA, Smith PD, Aylward E, Li Q, Chan M, Barta PE, Pearlson GD. Mesial temporal lobe measurements on magnetic resonance imaging scans. *Psychiatry Res*. 1998;83(2):85-94.
65. Lorensen WE, Cline HE. Marching cubes: a high resolution 3D surface construction algorithm. *Comput Graph (ACM)*. 1987;21(4):163-169. doi:10.1145/37402.37422.
66. Woods JI. *Semi-regular Mesh Extraction From Volumes* [master's thesis]. Pasadena: California Institute of Technology; 2000.
67. Kim NK, Kim HJ, Yoon SJ, Lyoo IK, Kang SH, Dager SR, Renshaw PF. Amygdala shape analysis and parametric surface visualization using iterative closest point algorithm and spherical mapping. *IEICE Technical Report*. 2007;106(509):271-274.
68. Amunts K, Kedo O, Kindler M, Pieperhoff P, Mohlberg H, Shah NJ, Habel U, Schneider F, Zilles K. Cytoarchitectonic mapping of the human amygdala, hippocampal region and entorhinal cortex: intersubject variability and probability maps. *Anat Embryol (Berl)*. 2005;210(5-6):343-352.
69. The SPM anatomy toolbox. Institut für Neurowissenschaften und Medizin (INM) Web site. [http://www.fz-juelich.de/inm/spm\\_anatomy\\_toolbox](http://www.fz-juelich.de/inm/spm_anatomy_toolbox). Accessed August 29, 2009.
70. Zilles K, Schleicher A, Palomero-Gallagher N, Amunts K. Quantitative analysis of cyto- and receptor architecture of the human brain. In: Toga AW, Mazziotta JC, eds. *Brain Mapping: The Methods*. 2nd ed. San Diego, CA: Academic Press; 2002.
71. Yang Y, Raine A, Narr KL, Colletti P, Toga AW. Localization of deformations within the amygdala in individuals with psychopathy. *Arch Gen Psychiatry*. 2009;66(9):986-994.
72. Herbert MR, Ziegler DA, Deutsch CK, O'Brien LM, Kennedy DN, Filipek PA, Bakardjiev AI, Hodgson J, Takeoka M, Makris N, Caviness VS Jr. Brain asymmetries in autism and developmental language disorder: a nested whole-brain analysis. *Brain*. 2005;128(pt 1):213-226.
73. Schumann CM, Barnes GC, Lord C, Courchesne E. Amygdala enlargement in toddlers with autism related to severity of social and communication impairments. *Biol Psychiatry*. 2009;66(10):942-949.
74. Benjamini Y, Hochberg Y. Controlling the false discovery rate: a practical and powerful approach to multiple testing. *J R Stat Soc Series B Stat Methodol*. 1995;57(1):289-300.
75. Hwang J, Lyoo IK, Dager SR, Friedman SD, Oh JS, Lee JY, Kim SJ, Dunner DL, Renshaw PF. Basal ganglia shape alterations in bipolar disorder. *Am J Psychiatry*. 2006;163(2):276-285.
76. Kirk RE. *Experimental Design: Procedures for the Behavioral Sciences*. 3rd ed. Pacific Grove, CA: Brooks/Cole Publishing Co; 1995.
77. Dziobek I, Fleck S, Rogers K, Wolf OT, Convit A. The 'amygdala theory of autism' revisited: linking structure to behavior. *Neuropsychologia*. 2006;44(10):1891-1899.
78. Amunts K, Schleicher A, Bürgel U, Mohlberg H, Uylings HB, Zilles K. Broca's region revisited: cytoarchitecture and intersubject variability. *J Comp Neurol*. 1999;412(2):319-341.
79. Amaral DG. The primate amygdala and the neurobiology of social behavior: implications for understanding social anxiety. *Biol Psychiatry*. 2002;51(1):11-17.
80. Sah P, Faber ES, Lopez De Armentia M, Power J. The amygdaloid complex: anatomy and physiology. *Physiol Rev*. 2003;83(3):803-834.
81. Baxter MG, Murray EA. The amygdala and reward. *Nat Rev Neurosci*. 2002;3(7):563-573.
82. Gottfried JA, O'Doherty J, Dolan RJ. Appetitive and aversive olfactory learning in humans studied using event-related functional magnetic resonance imaging. *J Neurosci*. 2002;22(24):10829-10837.
83. Miller SS, Spear NE. Olfactory learning in the rat neonate soon after birth. *Dev Psychobiol*. 2008;50(6):554-565.
84. Wolpert DM, Doya K, Kawato M. A unifying computational framework for motor control and social interaction. *Philos Trans R Soc Lond B Biol Sci*. 2003;358(1431):593-602.
85. Anderson AK, Christoff K, Stappen I, Panitz D, Ghahremani DG, Glover G, Gabrieli JD, Sobel N. Dissociated neural representations of intensity and valence in human olfaction. *Nat Neurosci*. 2003;6(2):196-202.
86. Quartz SR, Sejnowski TJ. The neural basis of cognitive development: a constructivist manifesto. *Behav Brain Sci*. 1997;20(4):537-556.
87. Wang K, Zhang H, Ma D, Bucan M, Glessner JT, Abrahams BS, Salyakina D, Imielinski M, Bradfield JP, Sleiman PM, Kim CE, Hou C, Frackelton E, Chia-vacci R, Takahashi N, Sakurai T, Rappaport E, Lajonchere CM, Munson J, Estes A, Korvatska O, Piven J, Sonnenblick LI, Alvarez Retuerto AI, Herman EI, Dong H, Hutman T, Sigman M, Ozonoff S, Klin A, Owley T, Sweeney JA, Brune CW, Cantor RM, Bernier R, Gilbert JR, Cuccaro ML, McMahon WM, Miller J, State MW, Wassink TH, Coon H, Levy SE, Schultz RT, Nurnberger JI, Haines JL, Sutcliffe JS, Cook EH, Minshew NJ, Buxbaum JD, Dawson G, Grant SF, Geschwind DH, Pericak-Vance MA, Schellenberg GD, Hakonarson H. Common genetic variants on 5p14.1 associate with autism spectrum disorders. *Nature*. 2009;459(7246):528-533.
88. Morrow EM, Yoo SY, Flavell SW, Kim TK, Lin Y, Hill RS, Mukaddes NM, Balkhy S, Gascon G, Hashmi A, Al-Saad S, Ware J, Joseph RM, Greenblatt R, Gleason D, Ertelt JA, Apse KA, Bodeil A, Partlow JN, Barry B, Yao H, Markianos K, Ferland RJ, Greenberg ME, Walsh CA. Identifying autism loci and genes by tracing recent shared ancestry. *Science*. 2008;321(5886):218-223.
89. Alarcón M, Abrahams BS, Stone JL, Duvall JA, Perederiy JV, Bomar JM, Sebat J, Wigler M, Martin CL, Ledbetter DH, Nelson SF, Cantor RM, Geschwind DH. Linkage, association, and gene-expression analyses identify CNTNAP2 as an autism-susceptibility gene. *Am J Hum Genet*. 2008;82(1):150-159.
90. Just MA, Cherkassky VL, Keller TA, Minshew NJ. Cortical activation and synchronization during sentence comprehension in high-functioning autism: evidence of underconnectivity. *Brain*. 2004;127(pt 8):1811-1821.
91. Koshino H, Kana RK, Keller TA, Cherkassky VL, Minshew NJ, Just MA. fMRI investigation of working memory for faces in autism: visual coding and underconnectivity with frontal areas. *Cereb Cortex*. 2008;18(2):289-300.
92. Markram K, Rinaldi T, La Mendola D, Sandi C, Markram H. Abnormal fear conditioning and amygdala processing in an animal model of autism. *Neuropsychopharmacology*. 2008;33(4):901-912.
93. McEwen BS. Protection and damage from acute and chronic stress: allostasis and allostatic overload and relevance to the pathophysiology of psychiatric disorders. *Ann N Y Acad Sci*. 2004;1032:1-7.
94. Bauman ML, Kemper TL. *The Neurobiology of Autism*. 2nd ed. Baltimore, MD: The Johns Hopkins University Press; 2005.
95. Amunts K, Zilles K. Atlases of the human brain: tools for functional neuroimaging. In: Zaborszky L, Wouterlood FG, Lanciego JL, eds. *Neuroanatomical Tract-Tracing 3: Molecules, Neurons, and Systems*. New York, NY: Springer; 2006.
96. Pieperhoff P, Hömke L, Schneider F, Habel U, Shah NJ, Zilles K, Amunts K. Deformation field morphometry reveals age-related structural differences between the brains of adults up to 51 years. *J Neurosci*. 2008;28(4):828-842.
97. Fischl B, Rajendran N, Busa E, Augustinack J, Hinds O, Yeo BT, Mohlberg H, Amunts K, Zilles K. Cortical folding patterns and predicting cytoarchitecture. *Cereb Cortex*. 2008;18(8):1973-1980.
98. Maljkovic A, Amunts K, Schleicher A, Mohlberg H, Eickhoff SB, Wilsch M, Palomero-Gallagher N, Armstrong E, Zilles K. Cytoarchitectonic analysis of the human extrastriate cortex in the region of V5/MT+: a probabilistic, stereotaxic map of area hOc5. *Cereb Cortex*. 2007;17(3):562-574.
99. Scheperjans F, Eickhoff SB, Hömke L, Mohlberg H, Hermann K, Amunts K, Zilles K. Probabilistic maps, morphometry, and variability of cytoarchitectonic areas in the human superior parietal cortex. *Cereb Cortex*. 2008;18(9):2141-2157.
100. Good CD, Johnsrude IS, Ashburner J, Henson RN, Friston KJ, Frackowiak RS. A voxel-based morphometric study of ageing in 465 normal adult human brains. *Neuroimage*. 2001;14(1, pt 1):21-36.
101. Keller SS, Wilke M, Wiesmann UC, Sluming VA, Roberts N. Comparison of standard and optimized voxel-based morphometry for analysis of brain changes associated with temporal lobe epilepsy. *Neuroimage*. 2004;23(3):860-868.
102. Allen JS, Bruss J, Brown CK, Damasio H. Normal neuroanatomical variation due to age: the major lobes and a parcellation of the temporal region. *Neurobiol Aging*. 2005;26(9):1245-1260.
103. Schumann CM, Amaral DG. Stereological estimation of the number of neurons in the human amygdaloid complex. *J Comp Neurol*. 2005;491(4):320-329.